

# Weierstraß-Institut für Angewandte Analysis und Stochastik

im Forschungsverbund Berlin e.V.

Preprint

ISSN 0946 – 8633

## A new model for passive mode-locking in a semiconductor laser

Andrei Vladimirov<sup>1</sup>, Dmitry Turaev<sup>2</sup>, Gregory Kozyreff<sup>3</sup>,

submitted: 25th November 2003

<sup>1</sup> Weierstrass Institute  
for Applied Analysis  
and Stochastics,  
Mohrenstrasse 39  
D - 10117 Berlin  
Germany  
E-Mail: vladimir@wias-berlin.de

<sup>2</sup> Ben Gurion University  
P.O.B. 653  
84105 Beer-Sheva  
Israel  
E-Mail: turaev@cs.bgu.ac.il

<sup>3</sup> OCIAM  
Mathematical Institute  
24-29 St.Giles'  
Oxford OX1 3LB  
United Kingdom  
E-Mail: kozyreff@math.ox.ac.uk

No. 893

Berlin 2003



---

2000 *Mathematics Subject Classification.* 78A60,34C23.

*Key words and phrases.* semiconductor laser, mode-locking, delay differential equations, bifurcations.

1999 *Physics and Astronomy Classification Scheme.* 42.60.Fc,42.55.Px,42.60.Mi,42.65.Pc,42.60.Gd.

Edited by  
Weierstraß-Institut für Angewandte Analysis und Stochastik (WIAS)  
Mohrenstraße 39  
10117 Berlin  
Germany

Fax: + 49 30 2044975  
E-Mail: [preprint@wias-berlin.de](mailto:preprint@wias-berlin.de)  
World Wide Web: <http://www.wias-berlin.de/>

## Abstract

We propose a new model for passive mode-locking that is a set of ordinary delay differential equations. We assume the ring cavity geometry and a Lorentzian spectral filtering of the pulses, but do not use small gain and loss and weak saturation approximations. By means of a continuation method we study mode-locking solutions and their stability. We found that stable mode-locking can exist even when the non-lasing state between pulses becomes unstable.

The passive mode-locking (ML) of lasers is a very effective technique to generate high quality short pulses with high repetition rates. Monolithic semiconductor lasers (SCL), passively or hybrid mode-locked, are ideal for applications in high speed telecommunications on account of their compactness, low cost, and reliability [1]. Large semiconductor material gain coefficients, short recovery times and small size of the device allow to achieve high repetition rates. The basic mechanism for passive ML is well understood since the analysis by New [2], who showed that the differential saturation of the gain and losses in the laser cavity opens a short temporal window of net gain for pulses. A wide range of experimental, numerical, and analytical methods exist to characterize ML (for an overview, see Haus[3] and Avrutin *et al.*[4]). While numerical integrations of travelling wave field equations coupled to material equations (distributed models) faithfully reproduce experimental observations, they offer little insight on the underlying dynamics. This is why analytical approaches based on lumped element models, mainly those introduced by New [2] and Haus [5, 6, 7, 8, 9] for slow and fast saturable absorbers, are still widely used. Inevitably, though, these approaches require certain approximations that in many cases are hardly satisfied in experiment. New, for instance, assumed small gain and loss per cavity round trip and ignored spectral filtering. Haus did take spectral filtering into consideration under the parabolic approximation and showed that even for an infinite bandwidth ML stability boundaries are different from that obtained by New [5]. In order to get analytical expression for ML pulse shape further approximations had to be made on the way, such as the assumption that the intra-cavity media are only slightly saturated. Yet, this leads to an agreement between analytical results and experimental data on the dye laser [8]. This success has prompted many studies of variations of Haus' model [4].

In this paper, we propose and discuss a new model for passive ML that is a set of ordinary delay differential equations (DDE). In doing so, we avoid the approximations of small gain and loss per cavity round trip and weak saturation; these do not hold well in SCL devices. On the other hand, as in most lumped element models,

we neglect the spatial effects inherent to a linear cavity, such as spatial hole burning and self-interference of the pulse near the mirrors. This amounts to consider a unidirectional lasing ring cavity. Absorbing, amplifying, and spectral filtering segments are placed in succession in the cavity. Using the lumped-element approach [4] the following equations governing the evolution of the field amplitude  $a(t)$  at the entrance of the absorber section, the gain  $g(t)$ , and the saturable losses  $q(t)$ , can be derived [10]:

$$a(t+T) = \sqrt{\kappa} \int_{-\infty}^t f(t-\theta) e^{\frac{1-i\alpha_g}{2}g(\theta) - \frac{1-i\alpha_q}{2}q(\theta)} a(\theta) d\theta, \quad (1)$$

$$\dot{g}(t) = J_g - \gamma_g g(t) - e^{-q(t)} (e^{g(t)} - 1) |a(t)|^2, \quad (2)$$

$$\dot{q}(t) = J_q - \gamma_q q(t) - s (1 - e^{-q(t)}) |a(t)|^2. \quad (3)$$

Here  $\alpha_r$ ,  $\gamma_r$ , and  $J_r$  ( $r = g, q$ ) are respectively the linewidth enhancement (self-phase modulation) factors, carrier density relaxation rates, and pump parameters for the gain and loss sections of the cavity. The cavity and semiconductor material dispersive effects are taken into account by the linear impulse response function  $f(t)$ ;  $\sqrt{\kappa} < 1$  is the linear attenuation factor per pass and  $T$  is the cold cavity round-trip time. In (2) and (3),  $|a(t)|^2$  is taken to be the pulse power divided by the saturation energy  $E_g$  of the amplification section, while  $s = E_g/E_q$  is the ratio of saturation energies of the gain and loss sections.

Typical monolithic devices comprise Bragg reflectors, whose frequency bandwidth is much narrower than that of the material gain. Hence, the spectral filtering of the cavity is mainly determined by the mirrors. We shall assume it to be Lorentzian, i.e.  $f(t) = \gamma e^{-\gamma t}$ . This is valid close enough to the main peak of the spectral reflectance and if the Bragg response is reactive only [11]. Equation (1) can then be replaced by the delay differential equation:

$$\gamma^{-1} \dot{a}(t) + a(t) = \sqrt{\kappa} e^{\frac{1-i\alpha_g}{2}g(t-T) - \frac{1-i\alpha_q}{2}q(t-T)} a(t-T). \quad (4)$$

Indeed, the general solution of (4) is given by  $a(t) = a(0) e^{-\gamma t} + \int_0^t e^{\gamma(\theta-t)} \text{rhs}(\theta-T) d\theta$ , where  $\text{rhs}(t-T)$  is the right hand side of (4), and it coincides with (1) provided that  $a(0) = \int_{-\infty}^0 e^{\gamma\theta} \text{rhs}(\theta-T) d\theta$ . Strictly speaking, Eq. (4) is equivalent to Eq. (1) only under this specific initial condition. However, since in the long time limit, the effect of initial condition on the solution decays exponentially in time, its precise form can be safely ignored.

Equations (2), (3), and (4) constitute the new model of this Letter. New's results [2] can be obtained by setting  $\gamma^{-1} \dot{a}(t) = 0$  in the left hand side of (4) and expanding exponentials in (4), (2), and (3) up to the first order terms in  $g$  and  $q$ , while Haus' master equation can be recovered in the limit  $\gamma T \rightarrow \infty$  by applying the same expansion together with the weak saturation approximation [10].

One advantage of this new formulation of the ML problem is that it allows us to make use of techniques that have been developed for DDE systems. From now on, for simplicity, we restrict our numerical analysis to the case when  $\alpha_{g,q} = 0$  in (4).

The constant intensity (cw) solution of (4), (2), and (3) exists above the linear threshold,  $J_g/\gamma_g > (J_q/\gamma_q - \ln \kappa)$ . Its bifurcation diagram is shown in Fig. 1 in the  $(J_g, J_q)$ -plane for the parameter values given in the figure caption. The curves  $H_n$  indicate Andronov-Hopf bifurcation to time-periodic intensity with period close to  $T/n$ . Thus, the curve  $H_1$  corresponds to the fundamental ML regime with pulse repetition frequency close to  $\Omega_1 = 2\pi/T$ , while the curves  $H_n$  with  $n = 2, 3, 4$  signal the onset of multiple pulse ML regimes with the repetition frequencies close to  $n\Omega_1$ . On the other hand,  $H_Q$  is an Andronov-Hopf bifurcation with a frequency approximately eight times smaller than  $\Omega_1$ . This bifurcation is responsible for the Q-switching instability.

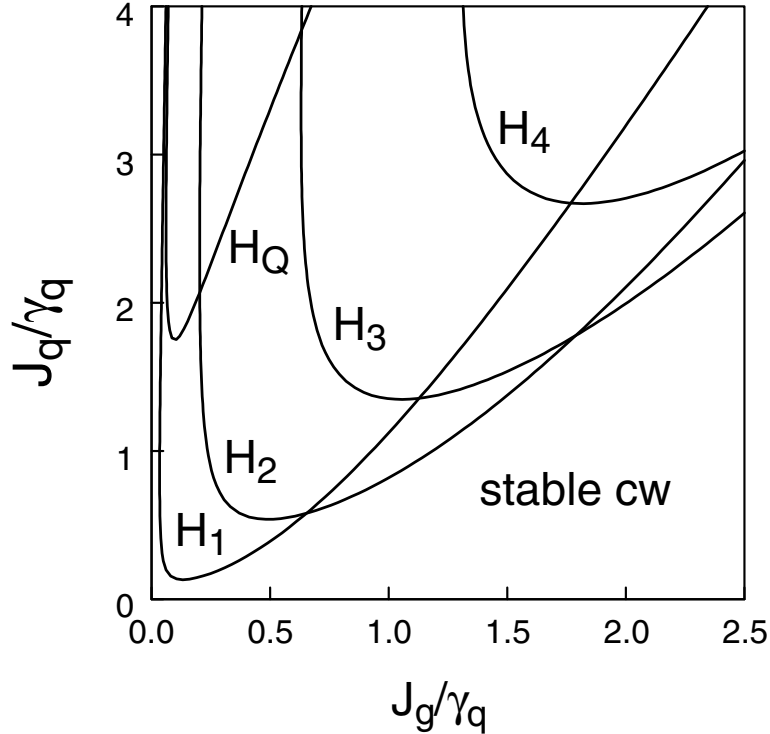


Figure 1: Andronov-Hopf bifurcations of the cw solution of Eqs. (2), (3), and (4). The parameters are:  $T = 25$  ps,  $\gamma^{-1} = 0.4$  ps,  $\alpha_{g,q} = 0$ ,  $s = 5$ ,  $\gamma_g^{-1} = 1$  ns,  $\gamma_q^{-1} = 10$  ps, and  $\kappa = 0.5$ .

Similarly to the Andronov-Hopf bifurcation curves the branches of periodic solutions and their stability have been calculated numerically using DDE-BIFTOOL [12]. The result is shown in Fig. 2 for  $J_q = 2\gamma_q$ . One can see from the figure that the branch  $P_1$  corresponding to the fundamental ML regime has two stability ranges. The first of them is very narrow and located near the left Andronov-Hopf bifurcation point at small values of  $J_g$  where the amplitude of  $P_1$  is small. The second stability range is limited by two bifurcation points. The left one is a secondary Andronov-Hopf bifurcation point labeled  $QP$ . This bifurcation produces a solution with quasiperi-

odic laser intensity that corresponds to a ML regime modulated by the Q-switching frequency. With the decrease of the pump parameter  $J_g$  below the  $QP$  point, the modulation depth grows. The right bifurcation point, labeled  $SN$ , is a saddle-node bifurcation whereby two periodic intensity solutions, one stable and another unstable, merge and disappear. The solutions corresponding to multiple pulse ML are labeled  $P_2$ , and  $P_3$  in Fig. 2. These solutions undergo bifurcations similar to those of the fundamental branch  $P_1$ . From Fig. 2 one can notice that bistability exists between different mode-locking regimes for some ranges of parameters.

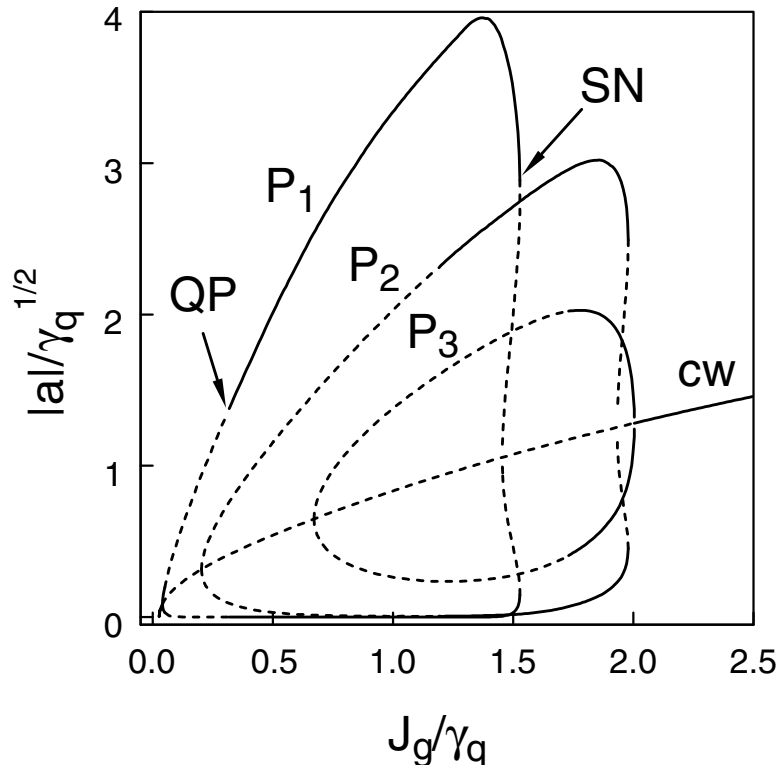


Figure 2: Branches of ML solutions bifurcating from the Andronov-Hopf bifurcation curves shown in Fig. 1. Solid (dotted) line indicate stable (unstable) solutions. The branch of constant intensity solutions is labeled  $cw$ .  $J_q = 2\gamma_q$ . Other parameters are the same as in Fig 1.

Fig. 3 illustrates stable time traces of the pulse intensity and the net gain per cavity round trip  $G = g - q + \ln \kappa$  for three different values of  $J_g$  on the  $P_1$  branch. Surprisingly, New’s stability criterion is only satisfied in Fig. 4b. This criterion stipulates that  $G < 0$  between pulses when  $|a|^2$  is small in order to prevent the growth of fluctuations on the wings of the pulses [2]. In other words, the zero intensity background has to be “stable” between pulses. However, Figs. 3a and 3c clearly contradict this point.

As it is seen from Fig. 3c, where the net gain window is opened well before the

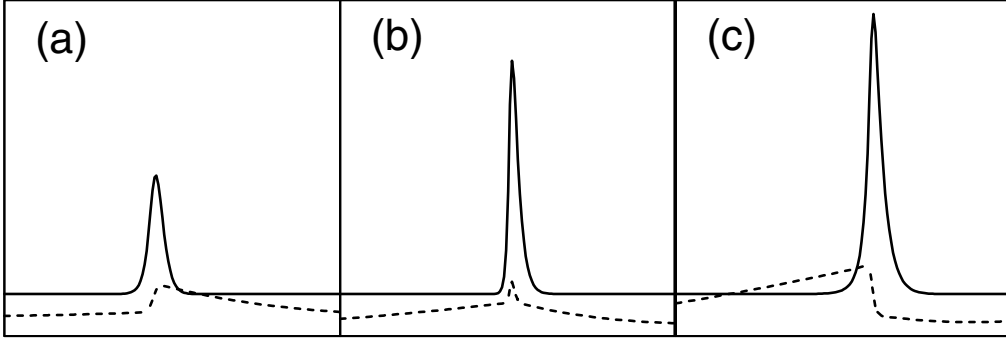


Figure 3: Time dependencies of the amplitude (solid line) of a fundamental ML pulse and the net gain parameter (dotted line). (a)  $J_g/\gamma_q = 0.4$ , (b)  $J_g/\gamma_q = 0.8$ , (c)  $J_g/\gamma_q = 1.32$ . The parameters are the same as in Fig 2.

arrival of a pulse in the course of the carrier density recovery process, ML solution can exhibit a behavior similar to that of the Q-switched laser with a saturable absorber [13]. This is a manifestation of delayed stability loss, a phenomenon that is typical of singularly perturbed dynamical systems. In dynamical terms, the phase space trajectory corresponding to a Q-switching regime spends most of the time between the pulses near the so-called slow manifold  $a = 0$ , passing from its stable part,  $G < 0$ , to the unstable one,  $G > 0$ . A pulse only starts to develop when the cumulative gain  $\int_{t_1}^{t_2} G(\theta) d\theta$  becomes positive, where  $(t_1, t_2)$  is the time interval spent near the slow manifold. This implies that  $G(t_2) > 0$ , i.e. similarly to the ML pulse shown in Fig. 3c, the Q-switching pulse has “unstable” background at the leading edge.

More generally, stable ML pulses with “unstable” background can exist due to the difference between the pulse group velocity  $v_p$  and the group velocity  $v_0$  of small perturbations. Consider a ML regime with the period  $T_p = T + \delta T$ , with  $\delta T \ll T$ . The group velocity of the pulse is then  $v_p = vT/T_p \approx v(1 - \delta T/T)$ , where  $v$  is the group velocity in the cold cavity. For small perturbations, we note that for  $\gamma T$  large enough,  $\dot{a}(t) + \gamma a(t) \approx \gamma a(t + \gamma^{-1})$  in the left hand side of (4). Equating this approximately to  $\gamma a(t - T)$ , we obtain a period  $T + \gamma^{-1}$ , which yields a velocity  $v_0 = v [1 - (\gamma T)^{-1}]$ . ML pulses with “unstable” leading edge shown in Fig. 3c are stable because they move faster than the perturbation (see Fig. 4). Similarly, the pulses with an “unstable” background on the trailing edge can be stable if they move slower than the perturbation, as for the parameter values of Fig. 3a. The latter situation was already noted by Paschotta and Keller[14].

To conclude, we have derived a DDE model for passive ML. Its extension to active or hybrid ML and inclusion of additional microscopic effects, e.g. carrier heating, is straightforward. This model is easy to simulate and analyze. It describes the appearance of ML pulses with “unstable” background, that are missing in the classical ML theories developed by New and Haus. Unlike the symmetric sech-pulses

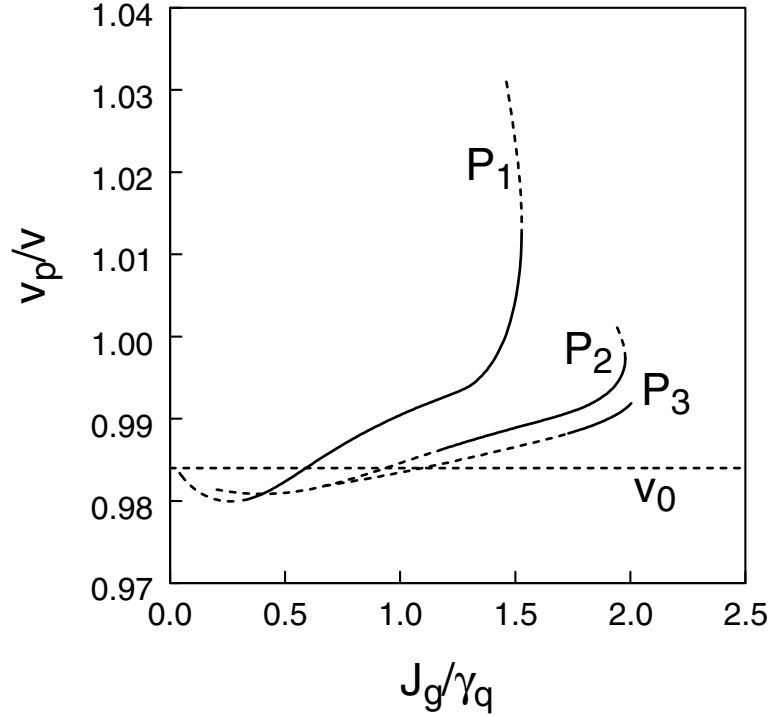


Figure 4: Group velocities of ML pulses divided by the cold cavity group velocity  $v$ . Dotted horizontal line represents the group velocity of small perturbations  $v_0$ . The parameters are the same as in Fig 2.

of the Haus theory, the pulses with “unstable” background are asymmetric and can exist in the case of high cavity losses [10],  $\kappa s < 1$ , i.e. in a situation typical of semiconductor lasers .

## References

- [1] P. Vasil’ev, *Ultrafast Diode Lasers: Fundamentals and Applications*, Artech House Publishers, 1995.
- [2] G.H.C. New, “Pulse evolution in mode-locked quasi-continuous lasers”, *IEEE J. QE-10*, 115-124 (1974).
- [3] H.Haus, “Modelocking of lasers“, *IEEE J. of Sel. Topics in Quantum Electronics*, **6**, 1173-1185 (2000).
- [4] E.A. Avrutin, J.H. Marsh, and E.L. Portnoi, “Monolithic and multi-GigaHertz mode-locked semiconductor lasers: Constructions, experiments, models and applications”, *IEE Proc.-Optoelectron.* **147**, 251 (2000).

- [5] H.Haus, “Theory of mode locking with a slow saturable absorber“, IEEE J. **QE-11**, 736-746 (1975);
- [6] H.Haus, “Modelocking of semiconductor laser diodes“, Jap. J. Appl. Phys. **20**, 1007-1020 (1981).
- [7] H.Haus, “Theory of mode locking with a fast saturable absorber“, J. Appl. Phys. **46**, 3049-3058 (1975).
- [8] H.A. Haus, C.V. Shank, and E.P. Ippen, “Shape of passively mode-locked laser pulses“, Optics Communications, **15**, 29-31 (1975).
- [9] J.C. Chen, H.A. Haus, and E.P. Ippen, “Stability of Lasers Mode Locked by Two Saturable Absorbers“, IEEE J. **QE 29**, 1228-1232 (1993).
- [10] A.G. Vladimirov and D. Turaev (unpublished).
- [11] S.L. McCall and P.M. Platzman, “An optimized  $\pi/2$  Distributed Feedback Laser“, IEEE J. **QE-21**, 1899-1904 (1985).
- [12] K. Engelborghs, T. Luzyanina, G. Samaey. DDE-BIFTOOL v. 2.00: a Matlab package for bifurcation analysis of delay differential equations. Technical Report TW-330, Department of Computer Science, K.U.Leuven, Leuven, Belgium, 2001.
- [13] T. Erneux, “Q-Switching bifurcation in a laser with a saturable absorber“, J. Opt. Soc. Am. B **5**, 1063-1069 (1988).
- [14] R. Paschotta and U. Keller, “Passive mode locking with slow saturable absorbers“, Appl. Phys. B **73**, 653-662 (2001).